Modelling of spall damage in ductile materials and its application to the simulation of plate impact on copper*

Zhang Feng-Guo(张凤国)†, Zhou Hong-Qiang(周洪强), Hu Jun(胡 军), Shao Jian-Li(邵建立), Zhang Guang-Ca(张广财), Hong Tao(洪 滔), and He Bin(何 斌)

Institute of Applied Physics and Computational Mathematics, Beijing 100094, *China*

(Received 17 November 2011; revised manuscript received 6 April 2012)

A statistical model of dynamic spall damage due to void nucleation and growth is proposed for ductile materials under intense loading, which takes into account inertia, elastic-plastic effect, and initial void size. To some extent, void interaction could be accounted for in this approach. Based on this model, the simulation of spall experiments for copper is performed with the Lagrangian finite element method. The simulation results are in good agreement with experimental data for the free surface velocity profile, stress record behind copper target, final porosity, and void concentrations across the target. The influence of elastic-plastic effect upon the damage evolution is explored. The correlation between the damage evolution and the history of the stress near the spall plane is also analyzed.

Keywords: spall damage, ductile materials, free surface velocity, plate impact

PACS: 46.50.+a, 46.40.–f **DOI:** 10.1088/1674-1056/21/9/094601

1. Introduction

The spall fracture, or impact-produced planar material separation, is the result of wave interactions that produce high dynamic tension within a particular region of the target material at a particular time. The dynamic tensile fracture of ductile metals is closely related to the nucleation, growth, and coalescence of voids. Many theoretical damage models, both empirical and micro-physical in nature, have been developed to describe and predict phenomenon of spall fracture, such as the Gurson model,[1] the Johnson model,[2] the nucleation and growth (NAG) model,[3] and the Bai model.[4] Some of these models are dependent on stress threshold, while others are dependent on strain threshold. Usually the damage level is quantified according to the void volume in the region of fracture for all these models. Up to now, there is not a general and satisfied spall model, and current models are confined in a narrow applicative range and should be further improved.[5] In addition, numerical analysis indicates that inertia, elastic-plastic effect, and initial void size have a significant influence on spallation damage.[6,7]

The statistical spall models are gradually developed and given more and more attention. Assuming the same void nucleation size, Tonks *et al.*[8] gave void nucleation expression related with stress and plastic strain, which succeeded in simulating tensile bar damage and plate impact experiment with void growth equation. Czarnota *et al.*[9] adopted a Weibull probability density function to describe the fluctuation of the nucleation pressure within the material. The void growth was described by a hollow sphere model with both micro-inertia effects and the matrix weakening due to void growth included. To some extent, void interaction could be accounted for in this approach. Simulations of free surface velocities for different impact velocities and different target thicknesses are found to be accurate for all test configurations.

In the present paper, the void nucleation model in NAG is used, assuming that nucleated voids are in the same size, and the voids of different sizes are formed in the evolution of the void nucleation produced in different times. The hollow sphere model is used to describe the evolution of the void, assuming the same ratio of the outer radius of the hollow spheres and their inner radius. Therefore, the evolution of the voids with different sizes can be described by a unified

*Project supported by the Science and Technology Development Foundation of China Academy of Engineering Physics (Grant Nos. 2009A09027 and 2009A09006).

†Corresponding author. E-mail: zhang_fengguo@iapcm.ac.cn

© 2012 Chinese Physical Society and IOP Publishing Ltd

porosity growth law. A new model is combined with the elastic-plastic hydrodynamic finite element code to simulate the plate impact test.

2. Dynamic damage evolution

2.1. Description of the material

All the voids will be deformed since they are produced in the damaged materials. In the deformation process, the voids are assumed to be spherical with a radius of a_i as shown in Fig. 1. They are embedded into spheres of an outer radius b_i made of matrix material, as shown in Fig. 2. The corresponding hollow sphere defines a unit cell, as shown in Fig. 3. The ratio of b_i to a_i is assumed to be identical for all unit cells, and the void interaction is indirectly taken into account. The evolution of this unit cell is based on the dynamic response of the hollow sphere subjected to a pressure loading according to the approach proposed by Carroll and Holt.[10]

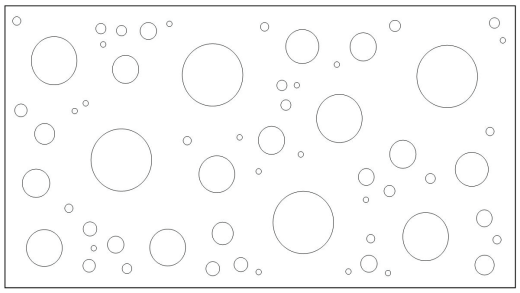


Fig. 1. Voids in damage material.

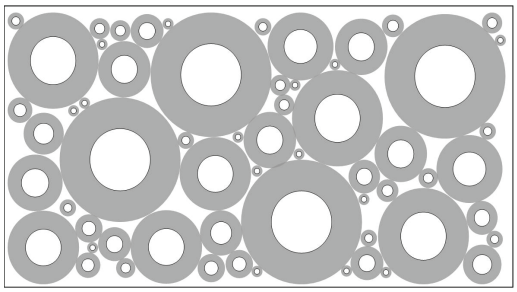


Fig. 2. Matrix material distributed over all voids. The ratio of the outer radius to the inner radius is identical for all unit cells.

2.2. Void evolution in the ductile materials

Johnson[2] suggested a very useful model of void growth under tensile loading condition in porous ductile materials, as shown in Fig. 3. In his model, the initial elastic and elastic–plastic phases of the evolution process were neglected, and only the fully plastic deformation around the void was considered in order to deal with the void growth in materials with very low initial porosities. Recent research on the mechanism of damage evolution clearly shows that early void growth, i.e., the elastic–plastic effect, plays an important role in the damage evolution, as pointed out by Molinari and Wright.[11] Since the void nucleation pressure is usually larger than material yield strength, the matrix material near the voids is in the plastic phase of the deformation process. Thus, let us first analyze the void growth in the elastic–plastic deformation around the void.

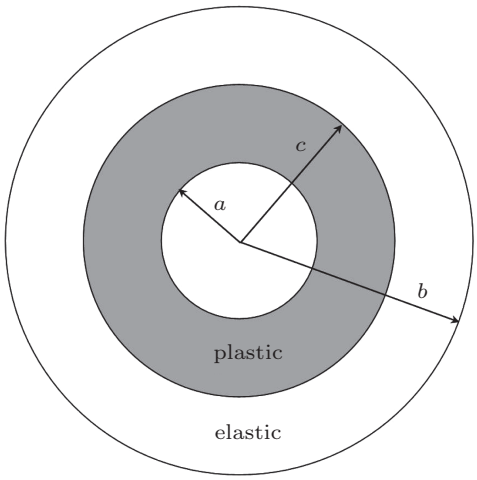


Fig. 3. Model of a porous material.

Figure 3 shows a simplified model of the porous material. For a single spherical void of radius a in a sphere of radius b subjected to the external stress $\sigma_r = \alpha p$, where p is a positive hydrostatic tension, and

$$\alpha = b^3/(b^3 - a^3). \tag{1}$$

Let a_0, b_0, and α_0 denote the initial values of a, b, and α, respectively, then the void evolution law can be written as[2]

$$\tau Q = \alpha p + 2\int_a^b \frac{\sigma_r - \sigma_\theta}{r}\,\mathrm{d}r, \tag{2}$$

where

$$\tau = \rho\frac{a_0^2}{3(\alpha_0 - 1)^{2/3}}, \tag{3}$$

$$Q(\ddot{\alpha}, \dot{\alpha}, \alpha) = \ddot{\alpha}[(\alpha - 1)^{-1/3} - \alpha^{-1/3}] - \frac{\dot{\alpha}^2}{6}[(\alpha - 1)^{-4/3} - \alpha^{-4/3}], \tag{4}$$

and ρ is the solid density, and σ_r and σ_θ are the radial and circumferential deviatoric stresses, respectively.

For the elastic region ($c < r \leq b$, see Fig. 3), let us consider the elastic deformation in the small strain limit. In this case, we have

$$\sigma_r - \sigma_\theta = 2GB(t)/r^3, \tag{5}$$

where G is the shear modulus of the solid, and

$$B(t) = a_0^3(\alpha_0 - \alpha)/(\alpha_0 - 1). \tag{6}$$

For the plastic region ($a < r \leq c$, see Fig. 3), the material is assumed to be elastic and viscoplastic so that

$$\sigma_r - \sigma_\theta = -Y_0 + \eta\dot{\gamma}^{\mathrm{p}}, \tag{7}$$

where $\dot{\gamma}^{\mathrm{p}}$ is the plastic shear strain rate, Y_0 the yield stress of the solid, and η the parameter of the material. Since the yield condition at the interface $r = c$ must be satisfied, we have

$$2GB(t)/c^3 = -Y_0 + \eta\dot{\gamma}^{\mathrm{p}}. \tag{8}$$

Neglecting the effect of plastic shear strain rate $\dot{\gamma}^{\mathrm{p}}$ and choosing

$$B(t)/c^3 \approx -Y_0/2G, \tag{9}$$

the spherical shell first becomes fully plastic with $c = b$, and we have

$$\alpha_{\mathrm{cr}} = 2G\alpha_0/(2G - Y_0). \tag{10}$$

Thus, for $\alpha \leq \alpha_{\mathrm{cr}}$, equation (1) can be rewritten as

$$\begin{aligned}
&\tau Q(\ddot{\alpha}, \dot{\alpha}, \alpha) \\
&= \alpha p(t) - \frac{4}{3}D_1 G\left(\frac{\alpha_0 - \alpha}{\alpha} + \frac{Y_0}{2G}\right) \\
&\quad - \frac{2}{3}D_2 Y_0 \ln\left(\frac{2G}{Y_0}\frac{\alpha - \alpha_0}{\alpha - 1}\right) \\
&\quad - \frac{2}{3}\frac{\dot{\alpha}}{\alpha - \alpha_0}\eta\left[\left(1 - \frac{Y_0}{2G}\right)^{1/3} - \left(1 - \frac{Y_0}{2G}\right)^{-2/3}\right. \\
&\quad \left. + \left(\frac{\alpha - 1}{\alpha_0 - 1}\right)^{2/3} - \left(\frac{\alpha - 1}{\alpha_0 - 1}\right)^{-1/3}\right],
\end{aligned} \tag{11}$$

and for $\alpha > \alpha_{\mathrm{cr}}$ it becomes

$$\begin{aligned}
&\tau Q(\ddot{\alpha}, \dot{\alpha}, \alpha) \\
&= \alpha p(t) - \frac{2}{3}D_2 Y_0 \ln\left(\frac{\alpha}{\alpha - 1}\right) - \frac{2}{3}\frac{\dot{\alpha}}{\alpha(\alpha - 1)}\eta \\
&\quad \times\left[\left(\alpha\frac{\alpha - 1}{\alpha_0 - 1}\right)^{2/3} - (\alpha - 1)\left(\frac{\alpha}{\alpha_0}\right)^{2/3}\right],
\end{aligned} \tag{12}$$

where D_1 and D_2 are model parameters. Equations (11) and (12) suggest that the growth of voids is determined only by a_0 and α. Assuming the same radius a_0 for all the void nucleation, the expansion of all hollow spheres with the same α can be described by Eqs. (11) and (12).

2.3. Porosity evolution

The porosity D is defined as the ratio of the total void volume V_α to the summation of the total void volume and matrix material volume V_{m}

$$D = V_\alpha/(V_{\mathrm{m}} + V_\alpha) = (1 - \alpha)/\alpha. \tag{13}$$

Thus, the dynamic evolution of the porosity is governed by

$$\dot{D} = \dot{\alpha}/\alpha^2. \tag{14}$$

2.4. Nucleation

Nucleation occurs when the new voids are added to the existing set. These new voids are presumed to have identical size a_0. In a unit solid volume, the number of voids nucleated is governed by the following nucleation rate function:[3]

$$\dot{N} = \begin{cases} \dot{N}_0 \exp[(p - p_0)/p_1], & p > p_0, \\ 0, & p \leq p_0, \end{cases} \tag{15}$$

where $\dot{N}_0$ and p_1 are material constants, and p_0 is the threshold for nucleation. The number N of voids and the volume of nucleated void ΔV_n in a time interval Δt are found to be

$$N = \dot{N}\Delta t, \tag{16}$$

$$\Delta V_n = 4\pi a_0^3 N/3. \tag{17}$$

2.4.1. Initial time of void nucleation

At the initial time of void nucleation, we have

$$\alpha = \Delta V_{\mathrm{n}} + 1, \tag{18}$$

and $D = D_0 = (\alpha - 1)/\alpha$. Assuming $\dot{\alpha} = 0$, $\ddot{\alpha} = 0$ at the initial time, equation (11) is rewritten as

$$\begin{aligned}
&\alpha p(t) - \frac{4}{3}D_1 G\left(\frac{\alpha_0 - \alpha}{\alpha} + \frac{Y_0}{2G}\right) \\
&\quad - \frac{2}{3}D_2 Y_0 \ln\left(\frac{2G}{Y_0}\frac{\alpha - \alpha_0}{\alpha - 1}\right) = 0.
\end{aligned} \tag{19}$$

The value of α_0 can be obtained from Eq. (19) by numerical analysis.

2.4.2. Influence of void nucleation on the porosity

For the change of material mass around void, the correlative physical quantities must be adjusted based upon the assumption that the volume of the void is preserved. For the change of void nucleation volume $\Delta V_{\rm n}$ in an interval, both α and α_0 will be changed into $\bar{\alpha}$ and $\bar{\alpha}_0$, which are described as

$$\bar{\alpha} = \Delta V_{\rm n} + \alpha, \tag{20}$$

$$\bar{\alpha}_0 = 1 + \left(\frac{\bar{\alpha}-1}{\alpha-1}\right)(\alpha_0 - 1). \tag{21}$$

According to the above definitions, α can be expressed as

$$\alpha = (V_{\rm m} + V_\alpha)/V_{\rm m}. \tag{22}$$

If the volume of the surrounding material is preserved, the growth rate of the present void volume is

$$\dot{V}_\alpha = V_{\rm m}\dot{\alpha}. \tag{23}$$

The change in the void volume is the sum of the contributions associated with nucleation and growth. In an interval Δt, it is

$$\Delta \bar{V}_\alpha = \dot{V}_\alpha \Delta t + \Delta V_{\rm n} V_{\rm m}. \tag{24}$$

Then, the new growth rate $\dot{\bar{V}}_\alpha$ of the void volume can be given by

$$\dot{\bar{V}}_\alpha = \frac{\Delta \bar{V}_\alpha}{\Delta t} = \dot{V}_\alpha + \frac{4\pi a_0^3 \dot{N}}{3} V_{\rm m}. \tag{25}$$

According to Eq. (23), the new growth law of $\dot{\bar{\alpha}}$ can be written as

$$\dot{\bar{\alpha}} = \dot{\alpha} + 4\pi a_0^3 \dot{N}/3. \tag{26}$$

The other physical quantities can be modified in a similar way.

2.5. The change of void volume

In the next interval with a new α, the void volume V changes to be

$$V^{n+1} = V^n(\alpha^{n+1} - 1)/(\alpha^n - 1). \tag{27}$$

Thus, according to Eqs. (16) and (27), we can obtain the number of voids in different size. It should be pointed out that, although the growth equation of α in all hollow spheres is the same, the growth laws of the voids are quite different.

2.6. The change of void number density

While calculating the void number density, the porosity in a virtual element is the same, i.e., voids of different sizes distribute uniformly in a virtual element. Thus, the number density n_i of void with radius a_i equals the void number N_i in virtual element divided by the distention of the cell, i.e.,

$$n_i = N_i/\alpha. \tag{28}$$

3. Pressure-porosity and stress-porosity relations

The stress-strain relations for material undergoing fracture must account for the presence of damage. As usual, the stress is separated into pressure and deviatoric components. The average pressure on the cross section of the fractured material can be related to the pressure in the solid components according to the following relation derived by Curran *et al.*[3] for porous material:

$$p = p_{\rm s}[\rho(1-D), E](1-D), \tag{29}$$

where E is the internal energy, and $p_{\rm s}$ is the mean stress in the solid material.

The yield strength reduces somewhat more rapidly than the modulus as the porosity increases, and it is adopted as follows:

$$Y = Y_0(1 - 4D), \tag{30}$$

where Y_0 is the yield strength for nonporous material.

4. Numerical results and comparison with experiments

Based on the proposed model, finite element simulations of plate impact tests are carried out to compare with the experiments on OFHC copper,[12] where a 2-mm-thick copper flyer plate impacts with a 9-mm-thick copper target at a velocity of 185 m/s. Both the simulation results and the experimental data for the free surface velocity profile are shown in Fig. 4. Comparison between them indicates that they are in good agreement. The model parameters determined by the simulation are $D_1 = 5.0$, $a_0 = 1.22$ μm, and $D_2 = 1.9$. The other parameters are given in Table 1.

Table 1. Representative material parameters of an OFHC copper.

ρ_0/kg·m^{-3}	G_0/GPa	Y_0/GPa	η(P)	Γ	$\dot{N}_0$/cm^{-3}·s^{-1}	p_0/GPa	p_1/GPa
8924	48.4	0.15	10	2.0	2.8×10^{12}	0.5	0.2

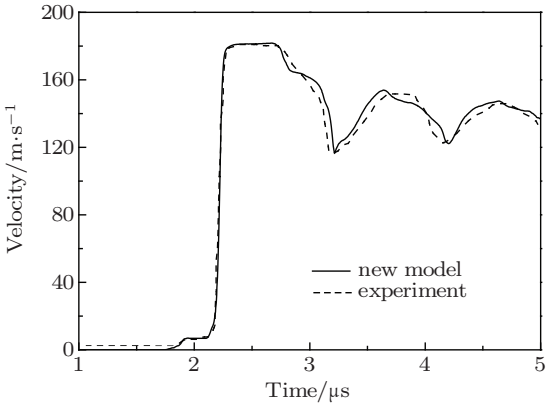


Fig. 4. Simulation result and experimental data of free surface velocity profiles.

In the experiment S24,[3] a 0.062-cm-thick copper flyer plate collides with a 0.159-cm-thick copper target plate at a velocity of 159 m/s. A simulation for the experiment is also performed with the previous material parameters and modeling parameters. Comparisons of the experimental data and the simulation results by the NAG model and our model for posttest porosity distributions, void concentrations through the thickness of the target, and the transmitted stress history in the PMMA backing plane are shown in Figs. 5–7, respectively. Obviously, the numerical results also agree very well with experiment data.

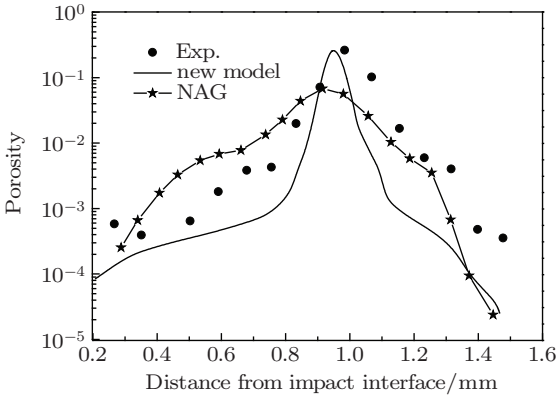


Fig. 5. Computed and observed damage (test S24).

Though we can simulate many experiment results using the NAG model, the NAG model is actually not appropriate when the number of the void changes.[13] Our proposed model not only solves this problem, but considers the effects of inertia, elastic–plastic deformation, and the initial size of void on the damage.[6] In summary, with the same set of material parameters and model parameters, good agreement of our results with experimental results for different physical quantities suggests that our model is suitable to investigate the spall damage.

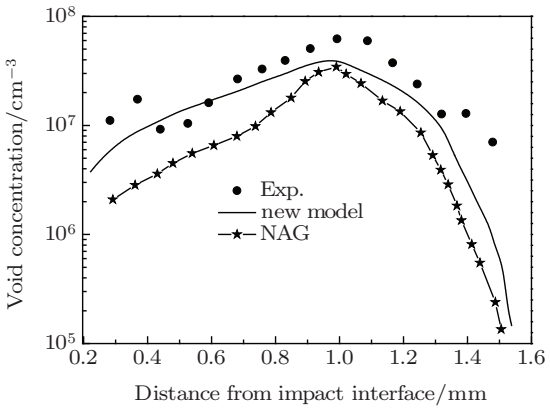


Fig. 6. Computed and observed void concentration (test S24).

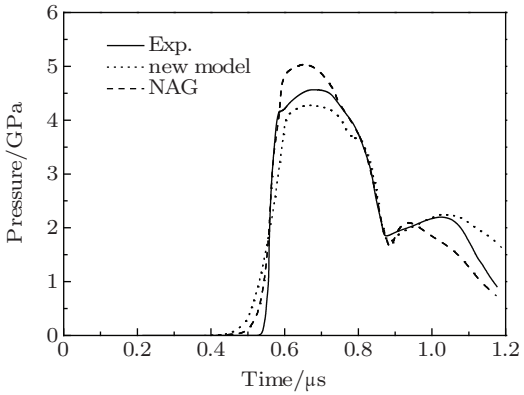


Fig. 7. Comparison of stress recorded at the manganin gage in PMMA behind OFHC copper with computed stress (test S24).

5. Numerical analysis of dynamic damage

The numerical analysis enables us to capture useful information such as pressure, strain rate, and porosity evolution inside the target, which cannot be obtained from experiments. Therefore, numerical simulations can help us obtain a deep insight into the

mechanism of spalling and a better interpretation of experimental measurements. Here our simulation is performed for the case of a 2-mm-thick copper flyer plate impacting a 9-mm-thick copper target plate at a velocity of 185 m/s.

The evolution of pressure is shown in Fig. 8. Obviously, the pressure increases linearly at first, then develops nonlinearly to reach a maximum value at about 2.77 μs, and finally decays rapidly. When the pressure maximum corresponding to $\alpha = \alpha_{\rm cr}$ is reached, matrix becomes fully plastic to be beneficial to the increase in void. The evolution of the porosity is also shown in Fig. 8. Obviously the porosity begins to grow very slowly with increasing pressure, and it increases rapidly after the maximum pressure is reached.

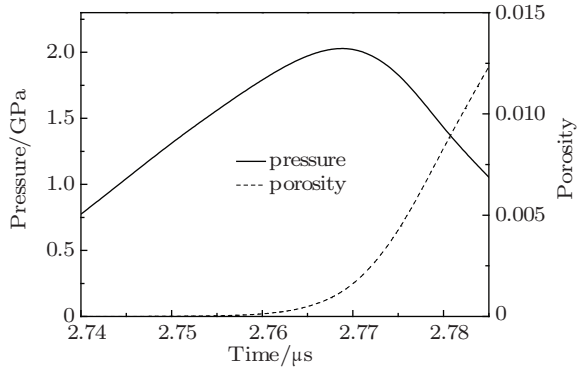


Fig. 8. Curves of tensile pressure and porosity versus time.

Comparison of Eq. (11) with Eq. (12) indicates that although the model parameter D_1 plays its role only in the elastic–plastic stage of void growth, it has direct influence upon the porosity evolution, as shown in Fig. 9. Thus, it is necessary to analyze the elastic–plastic effect in order to achieve a better description of the spall porosity evolution.

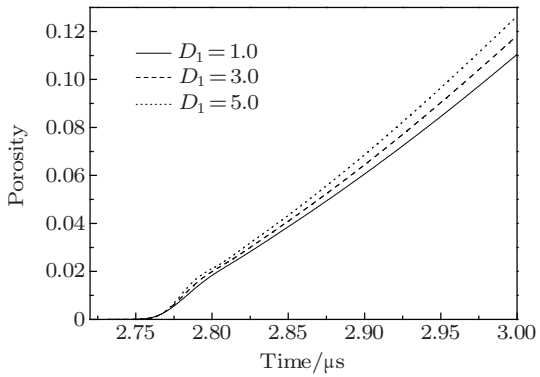


Fig. 9. Influence of parameter D_1 on the evolution of damage.

Metallographic observation shows that there is a great number of voids with different sizes in the damaged materials. Figure 10 shows the cumulative percentage of void volume and void numbers per unit volume varying with the void size in the spall plane. Obviously the number of the voids with a radius of about 11 μm is the biggest, and the majority of voids have a size from 8 to 11 μm, which has little contribution to the total void volume. Although the number of larger voids with the radius larger than 16 μm is small, they make greater contribution to the total void volume compared with those smaller voids.

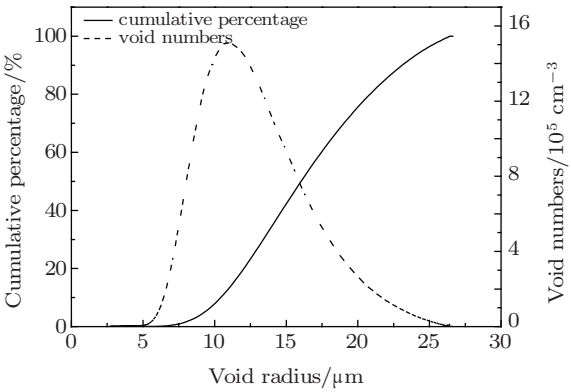


Fig. 10. Curves of the cumulative percentage of void volume and void numbers versus the void radius.

6. Conclusions

In this paper, a model of void nucleation, growth and void interactions has been proposed and used to characterize dynamic damage in ductile metals. The new dynamic damage model has been implemented in an elastic–plastic hydrodynamic finite element code to calculate the plate impact test. The free surface velocity profile, stress history behind target, final porosity and void number density through the thickness of the target are simulated with the same set of material parameters for different plate impact tests on the OFHC copper. All the results are in good agreement with the experiments

Based on the proposed model, the numerical results for plate impact show that the maximum tensile stress is related to the plastic deformation, the number of the voids with moderate size is the biggest, but the number of bigger voids can play a significant role in the porosity.

References

[1] Gurson A L 1977 *J. Eng. Mater. Technol.* **99** 2
[2] Johnson J N 1981 *J. Appl. Phys.* **52** 2812

[3] Curran D R, Seaman L and Shockey D A 1987 *Phys. Rep.* **147** 253

[4] Bai Y L, Bai J, Li H L, Ke F J and Xia M F 2000 *Int. J. Impact Eng.* **24** 685

[5] Chen X, Asay J R, Dwivedi S K and Field D P 2006 *J. Appl. Phys.* **99** 023528

[6] Zhang F G, Zhou H Q, Zhang G C and Hong T 2011 *Acta Phys. Sin.* **60** 074601 (in Chinese)

[7] Wang Y G, Hu J D, Qi M L and He H L 2011 *Acta Phys. Sin.* **60** 126201 (in Chinese)

[8] Tonks D L, Zurek A K, Thissell W R and Schwartz D S 2003 *Shock Compression of Condensed Matter* July 20-25, 2003 Portland, US, p. 507

[9] Czarnota C, Jacques N, Mercier S and Molinari A 2008 *J. Mech. Phys. Solids* **56** 1624

[10] Carroll M M and Holt A C 1972 *J. Appl. Phys.* **43** 1626

[11] Molinari A and Wright T W 2005 *J. Mech. Phys. Solids* **53** 1476

[12] Rajendran A M, Dietenberger M A and Grove D J 1989 *J. Appl. Phys.* **65** 1521

[13] Huang Z P, Yang L M and Pan K L 1993 *Adv. Mech.* **23** 433 (in Chinese)